Available online at www.sciencedirect.com

SciVerse ScienceDirect

Ceramics International 39 (2013) 6153–6163

CERAMICS INTERNATIONAL

www.elsevier.com/locate/ceramint

Road maps for processing foams containing particles

D.O. Vivaldini*, V.R. Salvini, A.P. Luz, V.C. Pandolfelli

Federal University of São Carlos, Materials Engineering Department, Materials Microstructure Engineering Group (GEMM), FIRE Associate Laboratory, Rod. Washington Luiz, km 235, São Carlos, SP 13565-905, Brazil

Received 29 October 2012; received in revised form 11 January 2013; accepted 12 January 2013
Available online 21 January 2013

Abstract

This work focuses on the development of tools for processing foams containing particles. By defining a foam stability index model and correlating it with the suspension viscosity, it was possible to build up a road map to indicate whether a suspension could or not result in high quality foams. The comparison of the literature data with predictions of the present model showed suitable agreement with the properties previously reported. It was also observed that by using the road map concept, foam systems can be understood better, which can lead to further innovative technologies.

Keywords: A. Suspension; Foam; Road map; Stability index

1. Introduction

In recent years, there has been great interest in foam and foam-like systems containing particles, which are present in many industrial sectors from mineral flotation to insulating materials and slag foaming [1]. Those systems usually present an outstanding long-term stability compared to common surfactant generated foams [2] as the particles are located on the film between the bubbles. However, a common technical issue in most applications is the lack of understanding of the fundamental concepts defining the foaminess/stability of the bubbles and its correlation with the particle present, regarding its size and chemical nature. Filling this gap could generate new insights resulting in technology advances and further innovations, either in well established areas (such as flotation and insulating foams) or related novel ones (slag foaming).

Some previous models have been derived in an attempt to describe those systems [3–5], but none of them was successful enough to incorporate the many different parameters that influence the overall foam stability.

Thus, the aim of this work is to design "Processing Road Maps" involving the most important variables leading to bubble stability. Fig. 1 shows an illustration where equations defining both axes (X and Y) would be the ultimate target of this work.

It must be highlighted that the road map concept was based on Ashby's materials selection methodology [6], which is often used to describe complex engineering systems by developing mathematical and (especially) graphical tools to quantify and compare different materials regarding their effectiveness for a specific application. That is exactly what the foaminess/stability of suspensions problem is in need of.

The next sections present the main variables that influence bubble stability and, based on some correlations among them, indexes (for the X and Y axes in Fig. 1) will be proposed:

- Firstly, the maximum capillary pressure that the bubble film can withstand ($P_{C\ max}$) and the total internal effective bubble pressure (ΔP_{eff}) are discussed.
- Secondly, the relationship between the adsorption free energy (ΔG_{ads}) of the particles at the bubble interface regarding their thermal energy ($K_B T$) is shown in order to better understand the adsorption stability.

The mathematical reasoning for the derivation of a foaminess/stability index expressed by the four variables

*Corresponding author. Tel.: +55 16 33518253; fax: +55 16 33615404.
E-mail addresses: diogoem05@gmail.com, diogoem05@yahoo.com.br (D.O. Vivaldini), vicpando@ufscar.br (V.C. Pandolfelli).

0272-8842/$ - see front matter © 2013 Elsevier Ltd and Techna Group S.r.l. All rights reserved.
http://dx.doi.org/10.1016/j.ceramint.2013.01.034

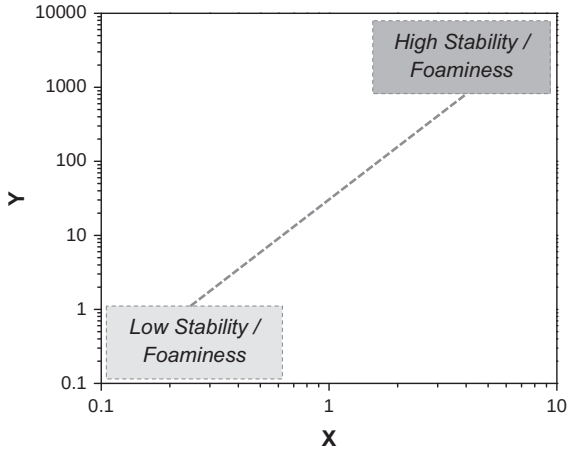

Fig. 1. Envisioned processing road map for the quantification and comparison of different particle stabilized foams regarding their stability and foam capacity (foaminess).

mentioned above ($P_{C\ max}$, ΔP_{eff}, ΔG_{ads}, K_BT) is also presented in this work, which could be suitable to describe the Y axis. It is also important to understand that both the bubble film thickness stability (expressed by the relationship between the $P_{C\ max}$ and the ΔP_{eff}) and the particle's adsorption stability on the bubble's interface (defined by the ΔG_{ads} and K_BT variables) are fundamental aspects of foams containing particles and they must be simultaneously attained. Furthermore, the X axis could be described by a rheological property, especially if the foam production technique is mechanical frothing, that could better address the constraints associated to the air incorporation in a suspension. The most accessible rheological data for foam systems is the viscosity of the suspension prior foaming. Hence, the viscosity, or an equation comprising it could expand the understanding providing a clearer vision toward foam systems, as will be discussed below.

2. $P_{C\ max}$, ΔP_{eff} and their correlation with the bubble film stability

The particles placed at the bubble interface can result in different structures (monolayer, bilayer, multilayer, etc.) which, along with other variables (wetting angle, for instance), define the "film strength" or the maximum capillary pressure it can withstand before becoming unstable. Based on the literature [7], the "intrinsic strength of the film" will henceforth be called maximum capillary pressure ($P_{C\ max}$) which is expressed in megapascal (10^6 N/m^2). There are many equations aiming to quantify this variable [4,7,8], however the one proposed by Kaptay [3], was selected by the authors to use in the present work, is given below.

$$P_{C\ max} = \frac{4f\gamma}{R_P}(\cos\theta + Z) \quad (1)$$

where, f is the fraction area of the bubble's surface that is coated by particles, θ is the wetting angle of the particles (deg.), R_p is the particle's radius (m), γ is the surface tension (N/m) of the gas–liquid interface and Z is a parameter related to the sort of particle configuration within the film. Additionally, it must be highlighted that $P_{C\ max}$ *is not a function of the bubble size*.

In order to evaluate whether a bubble is stable or not, one has to compare the strength of the film (which withstands the whole foam structure) with the stresses that the system is subjected to. Those stresses are mainly expressed by the effective pressure (ΔP_{eff}) acting over the bubbles and it can be calculated according to the following equation [3], also derived by Kaptay:

$$\Delta P_{eff} = \left(P_{atm} + \frac{2\gamma}{R_B} + \rho g H\right)\left[1 - f\left(1 - \cos^2\theta\right)\right] \quad (2)$$

where, P_{atm} is the atmospheric pressure (0.101 MPa), ρ the density (kg/m^3) of the system, g the acceleration due to the gravity (m/s^2), H the height (m) of the foam column and $2R_B$ the bubble diameter (m). The term ρgH in Eq. (2) is also known as the hydraulic pressure. The Laplace pressure due to the radius of curvature of the bubble is considered in the $2\gamma/R_B$ term. One can notice that Eq. (2) *is not a function of the particles size at the bubble's film*. Furthermore, it must be pointed out that the ΔP_{eff} represents the pressure developed inside the bubbles that could result in the rupture of the bubble's film and, thus, the foam collapse.

The interaction between $P_{C\ max}$ and ΔP_{eff} is expressed in Fig. 2 where the results of Eqs. (1) and (2) are shown for an aqueous system.

By analyzing Fig. 2, the following hypothesis can be stated:

I. There is a threshold for the $2R_p$ value, above which no bubble, regardless of its size, can be stable, as the $P_{C\ max}$ value will always be lower than the total internal

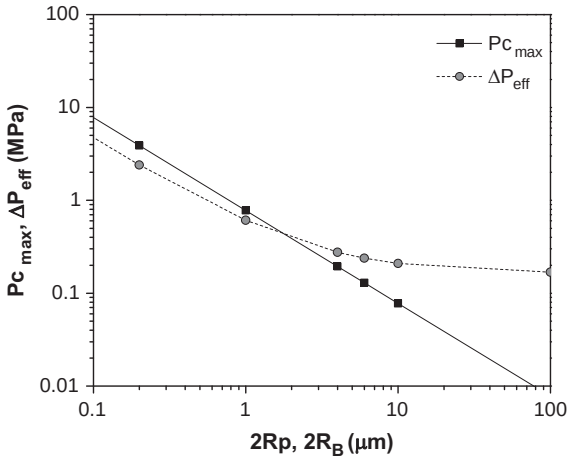

Fig. 2. $P_{C\ max}$ and ΔP_{eff} as a function of the bubble diameter (related to the ΔP_{eff} curve) and of the particle diameter (related to the $P_{C\ max}$ straight line). $\gamma = 0.072$ N/m, $f = 0.9$, $z = 0.633$, $\theta = 30°$, $H = 0.1$ m, $g = 9.8$ m/s^2 and $\rho = 1000$ kg/m^3.

pressure of the bubble (ΔP_{eff}). As presented in Fig. 2, that threshold seems to be close to 2 μm, although this value will depend on those variables inserted in both Eqs. (1) and (2).

II. The Laplace pressure ($2\gamma/R_B$ term) is the main source of the increase of the ΔP_{eff} value when $2R_B$ becomes lower than approximately 20 μm. This can indicate the difficulty of keeping bubbles below that size, as ΔP_{eff} increases steeply with the $2R_B$ decrease.

The fraction area of the bubble's surface coated by the particles (f) is another variable that plays an important role in the bubble stability. The $P_{C\,max}$ results are shown in Fig. 3, for three given f values (0.2, 0.4 and 0.9) and for $2R_p = 1$ μm. Thus, straight lines are generated as $P_{C\,max}$ does not depend on $2R_B$.

According to Fig. 3, one can realize that f is a major variable regarding the foam system stability. For $f < 0.2$, no bubble should be stable, assuming the parameter's values considered in Figs. 2 and 3. This result is in agreement with the work carried out by Gonzenbach et al. [9]. When those authors considered lower volume fraction (vol%) of particles to produce aqueous foams, they found out that the resulting bubbles were much bigger than those with high particle content. Based on Fig. 3, for a particle–liquid–bubble system to remain stable (regardless of its θ and γ values) the fraction area of bubbles coated by particles must be higher than 0.2. Therefore, the system has to generate bubble sizes that are compatible with the number of particles (related to the particle's volume fraction and particle size) so that f remains high. Considering a small amount of particles present in the suspension, if one is willing to generate a foam with high air volume fraction (P) and small bubble size ($2R_B$), this would only be accomplished when the f value is high, because the particles would have to be scattered over a large air-water interface. Nevertheless, as shown by Gonzenbach et al. [9], in such conditions bigger bubbles are formed as there is much less air–water interface to be coated by particles and, thus f could be high enough to stabilize the foam.

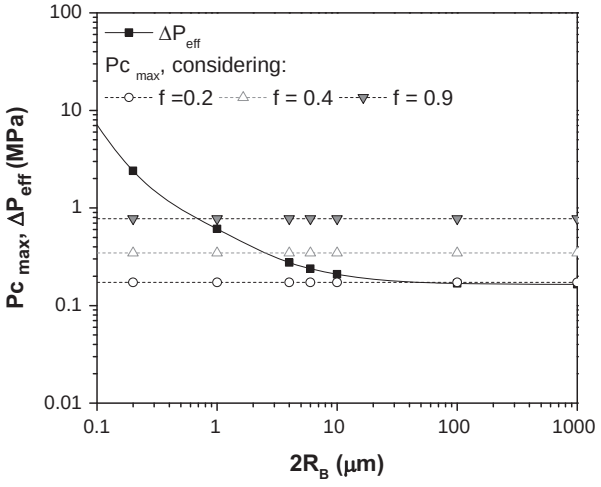

Fig. 3. Effect of f, the fraction area of the bubble's surface coated by particles, on the bubble's stability of an aqueous system. $P_{C\,max}$ results were generated for a fixed particle size ($2R_p = 1$ μm). The values used for the other variables were the same as presented in Fig. 2. The ΔP_{eff} curve was calculated for a fixed f value (0.6), as this parameter presents minor changes with f variations.

In Fig. 3, it is also important to notice the trend of the ($P_{C\,max} - \Delta P_{eff}$) difference. The value and modulus of the ($P_{C\,max} - \Delta P_{eff}$) difference change with $2R_B$, and when ($P_{C\,max} - \Delta P_{eff}$) < 0 an unstable system should be obtained, whereas the opposite condition indicates stability. For instance, considering the ΔP_{eff} and the $P_{C\,max}$ curves for $f = 0.4$ in Fig. 3, one can state that there is a threshold value for $2R_B$ below in which the $P_{C\,max} - \Delta P_{eff}$ is negative, representing an unstable condition. Above the $2R_B$ threshold, $P_{C\,max} - \Delta P_{eff}$ value is positive and the difference increases with $2R_B$ until a plateau is reached (when $2R_B$ is bigger than approximately 200 μm) whose value also depends on f. Therefore, the $P_{C\,max} - \Delta P_{eff}$ value is an indicative of the stability of the foam system.

In order to clarify the concepts described above, the $P_{C\,max} - \Delta P_{eff}$ difference was plotted as a function of the particle diameter for a fixed bubble size of 10 μm (Fig. 4a). On the other hand, Fig. 4b presents the same difference as a function of bubble size for a constant particle size of 1 μm.

Fig. 4a shows an interesting aspect which can also be observed in Fig. 3. $P_{C\,max} - \Delta P_{eff}$ plot becomes negative above a certain particle size (in the case of Fig. 4a, the threshold is approximately 4 μm), defining an *upper limit* for the particle size that results in stable foam films. On the other hand, Fig. 4b shows a threshold which indicates the *lower limit* for the bubble size that can be present in order to have a stable system.

Fig. 4a and b raises the question about the geometrical relationship between particles and bubbles, pointing out that another interesting way to understand the particle–bubble stability is to calculate the $P_{C\,max} - \Delta P_{eff}$ difference as a function of C, which is the mathematical ratio between $2R_p$ and $2R_B$ ($C = 2R_P/2R_B$) (Fig. 5).

Fig. 5 expands the understanding of the foam system as it shows that the C ratio defines the bubbles stability. It is possible to observe that as the C value decreases, the threshold value for the maximum stable bubble size increases and, given a fixed stable bubble size, the modulus of the $P_{C\,max} - \Delta P_{eff}$ difference also increases. Furthermore, when the C value is 2 (particles have twice the size of the bubbles), no foam configuration (bubble size) should attain stability, as the $P_{C\,max} - \Delta P_{eff}$ difference is always negative, regardless of the bubble size.

3. Adsorption of particles (ΔG_{ads}) normalized by their thermal energy

The bubble's film stability criterion is not the only factor that defines the overall stability of a foam containing particles.

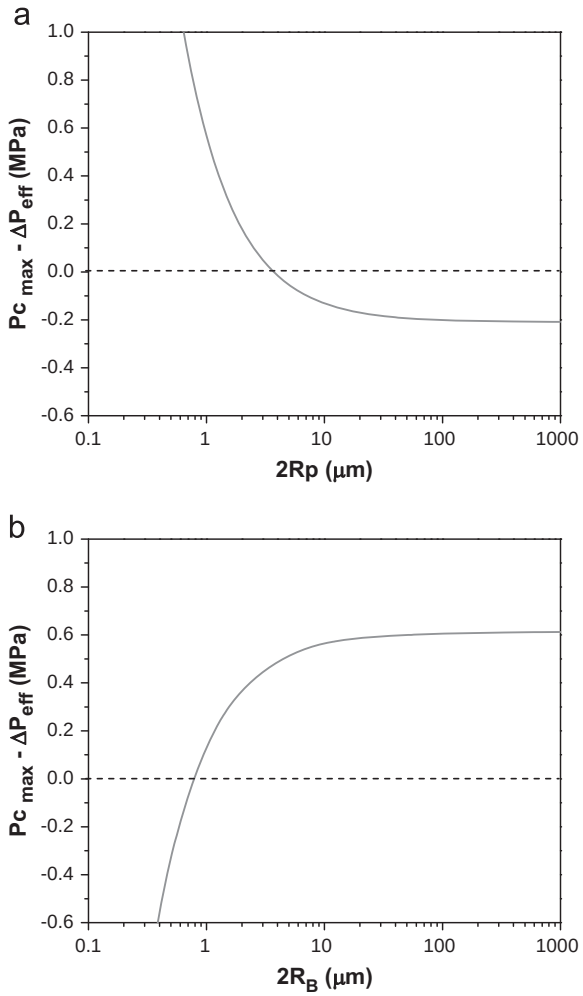

Fig. 4. (a) $P_{C\,max}-\Delta P_{eff}$ as a function of the particle size ($2R_p$) for a 10 μm diameter bubble ($2R_B$). (b) $P_{C\,max}-\Delta P_{eff}$ as a function of bubble size ($2R_B$) for 1 μm particle size ($2R_p$). The other variable values were kept the same as described in Fig. 2.

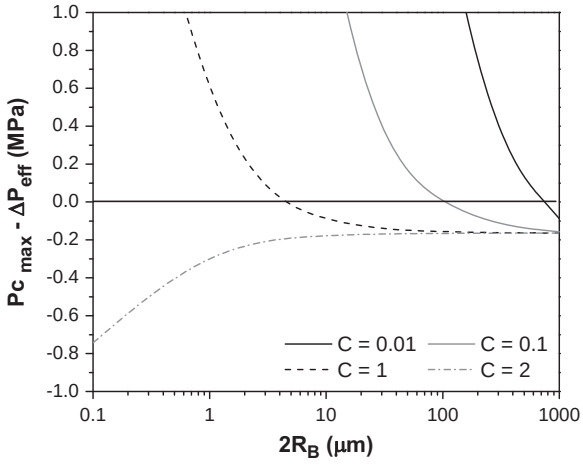

Fig. 5. $P_{C\,max}-\Delta P_{eff}$ as a function of $2R_B$ and C. The parameters used to calculate $P_{C\,max}$ were kept the same as described in Fig. 2.

Another very important aspect is the adsorption of particles at the gas–liquid interface. This concept is analogous to the geometrical limit criteria for particle-stabilized foams [10], as they state that the foam must have stability over its volume (within its film and over its gas–liquid interface regions), which is induced by the particles when they are present in the liquid. In other words, the foam cannot have a stable bubble film and an unstable liquid–gas interface, as both need to be attained.

When a particle is attached to a gas–liquid interface, the overall Gibbs free energy of the system is reduced, which makes this process thermodynamically favorable. The energy decrease due to this adsorption process at a flat interface can be mathematically described by Eq. (3) [2,11], when $0^\circ \le \theta \le 90^\circ$.

$$\Delta G_{ads} = \pi R_P{}^2 \gamma (1-\cos\theta)^2 \tag{3}$$

where ΔG_{ads} is expressed in Joules (J).

Nevertheless, the ΔG_{ads} value cannot be used to state whether the interface is stable or not. That argument can only be sustained when the energy released due to adsorption of the particles is compared to their own thermal energy, which is the origin of the Brownian motion of colloidal particles in suspension [12]. If the thermal energy value is close to the adsorption energy one, then the adsorption may not be carried out as the particles will have enough energy to break loose from the bubble's film.

The thermal energy of suspended colloidal particles is described by the product of the Boltzmann constant (K_B) and the absolute temperature (T) [13]. Therefore, by this estimative (K_BT), also expressed in Joules (J), the stability of the particles adsorption at the gas–liquid interface can be defined

$$\text{Interface stability} = \frac{\Delta G_{ads}}{K_B T} = \frac{\text{adsorption energy}}{\text{thermal energy}} \tag{4}$$

In Eq. (4), the influence of R_p and θ on the particles adsorption stability can be evaluated. Fig. 6 shows the results attained for an aqueous low temperature system.

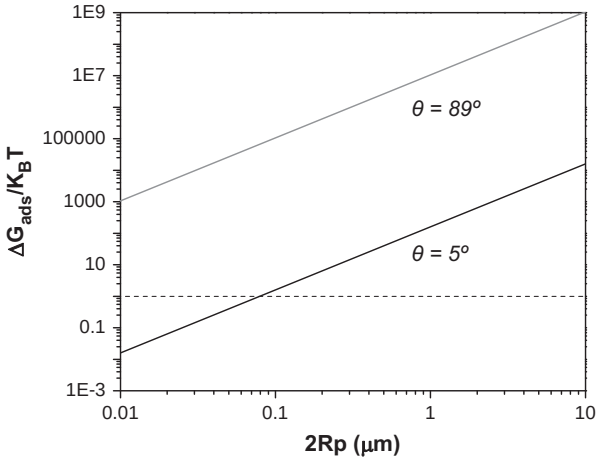

Fig. 6. Adsorption stability ($\Delta G_{ads}/K_BT$) as a function of the particle size ($2R_p$) and the wetting angle ($\theta = 5^\circ$ or 89°). The calculations were carried out assuming a constant temperature (373 K) and $\gamma = 0.072$ N/m. The dotted horizontal line represents ($\Delta G_{ads}/K_BT$) = 1.

Fig. 6 provides important insights about the interface stability which can be highlighted as follows:

I. The wetting angle (θ) shows a great influence on the stability of the particles adsorption process, as a five order of magnitude change in the $\Delta G_{ads}/K_B T$ ratio is observed when θ increases from 5° to 89°.
II. The particle size ($2R_p$) also affects the system's stability and for very hydrophilic particles ($\theta=5°$) there are particle size ranges that result in very low adsorption stability. As a matter of fact, there is a minimum threshold (approximately 0.07 μm) below which $\Delta G_{ads}/K_B T$ ratio <1, indicating a very unstable adsorption. This could be the reason that colloidal hydrophilic particles (such as colloidal silica) cannot give rise to stable foams [14,15].

4. Further steps toward a foaming/stability index

The stability index proposed in this work is an attempt to generate a theoretical tool aiming to draw a comparative analysis among foam systems. Therefore, the values attained should not be taken as absolute ones, instead they are suitable to carry out comparative analysis and provide trends for experimental procedures.

In order to combine the results obtained so far, the viability to attain a mathematical selection index was considered using the set of variables described in the previous sections, as they are related to the stability of the foam.

The next approach to the issue was to generate an equation that is able to connect the $P_{C\,max}-\Delta P_{eff}$ difference and the $\Delta G_{ads}/K_B T$ ratio. It must be highlighted that when $P_{C\,max}-\Delta P_{eff}$ becomes negative, a threshold for the stability of the foam should be observed. Therefore, the negative sign of the difference is shown if the index is calculated according to the following equation.

$$\text{Stability index} = (P_{C\,max}-\Delta P_{eff})\frac{\Delta G_{ads}}{K_B T} \quad (5)$$

In order to make the analysis and the results presentation easier, it was assumed that when the stability index became negative, it was made equal to zero. Therefore, in such conditions no possible stable foam system could be attained.

The product of ($P_{C\,max}-\Delta P_{eff}$) difference and $\Delta G_{ads}/K_B T$ ratio arises from the probability theory [16] which states that when two events are required to *take place simultaneously*, then the probabilities of each one must be multiplied: the ($P_{C\,max}-\Delta P_{eff}$) difference can be visualized as a probability associated to the bubble's film stability, whereas the $\Delta G_{ads}/K_B T$ ratio as the likelihood to attain stable particle adsorption at the bubbles interface.

Kaptay developed a similar concept to the stability index presented in Eq. (5) [25]. The author generated an equation by multiplying the $P_{C\,max}$ term and the $(1-\cos\theta)^2$ one, contained in Eq. (3). By his model, it is possible to calculate the stability of a system only as a function of θ, although no correlation with experimental data was provided. Hence, it is possible to state that Eq. (5) addresses the stability of a particle containing foam in a much broader way, by taking into account a higher number of relevant variables, therefore, resulting in a novel mathematical tool to investigate particle containing foam systems.

Fig. 7 shows the results obtained by applying Eq. (5) for hydrophilic ($\theta=5°$) and hydrophobic ($\theta=90°$) particles, respectively. These graphs also present the influence of the particle diameter over the stability of the foam. As mentioned above, there is a critical maximum particle size that can result in stable foams, which also depends on the bubble size ($2R_B$). It can be observed that the absolute value of the stability index is much higher for the more hydrophobic particles, mainly due to the much higher $\Delta G_{ads}/K_B T$ ratio. Furthermore, the critical particle size, above which the stability index is zero, is also higher for

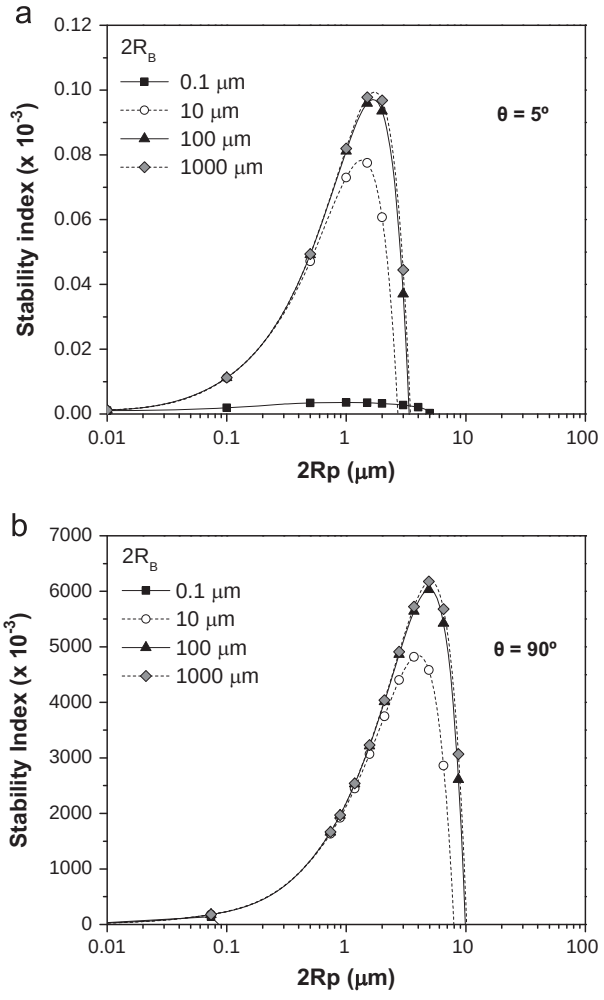

Fig. 7. Stability index (defined by Eq. (5)) as a function of the particle diameter ($2R_p$) and the bubble size ($2R_B$). The contact angle was fixed at 5° in (a), which characterizes highly hydrophilic particles, whereas in (b) θ was 90°, which indicates partially hydrophobic particles. The other variables were set as $f=0.9$, $z=0.405$ and $\gamma=0.072$ N/m, $H=0.1$ m, $g=9.8$ m/s^2 and $\rho=1000$ kg/m^3.

the hydrophobic particles, as it increases slightly when θ changes from 5° (~4 μm) to 90° (~10 μm).

An interesting feature observed in Fig. 7 is that the difference between the stability index values for the 10, 100 and 1000 μm bubbles begin to diverge only above a certain particles size (~1 μm), and the bigger the bubbles the more stable they are (higher stability index). This might imply that by using particles with a size below that threshold (< 1 μm), it would be easier to produce, for example, 10 μm bubbles, as there is no stability advantage associated by producing bigger bubbles.

Fig. 8 shows the results of Eq. (5) for a fixed bubble size diameter (0.1 μm). It can be observed that highly hydrophilic ($\theta = 5°$) particles can hardly stabilize foams even with bigger particles due to the lower overall stability index (~5 orders of magnitude lower than for $\theta = 90°$). This result is mainly a consequence of the low adsorption energy ($\Delta G_{ads}/K_B T$) of this system, as shown previously in Section 3. It is also possible to notice that the stability difference between particles presenting θ in the range of 70° and 90° is not as big as it is between the 5° curve profile (neither the absolute index values nor the particle diameter threshold). Therefore, the 70° and 90° plots are much more similar to each other when compared to the 5° one.

Fig. 9 shows the results for the stability index as a function of θ and $2R_B$ for 2 and 0.5 μm particle sizes, respectively.

For both the 2 μm and 0.5 μm particles, it can be observed that there is a suitable θ value (~85–90°) that provides the highest stability to the system.

Fig. 10 shows the stability index as a function of θ and of the particle size, given a fixed (10 μm) bubble size. It is interesting to observe that for a specific θ value, the optimized particle size changes.

The stability index defined by Eq. (5) appears to be a suitable mathematical method to describe the complexity

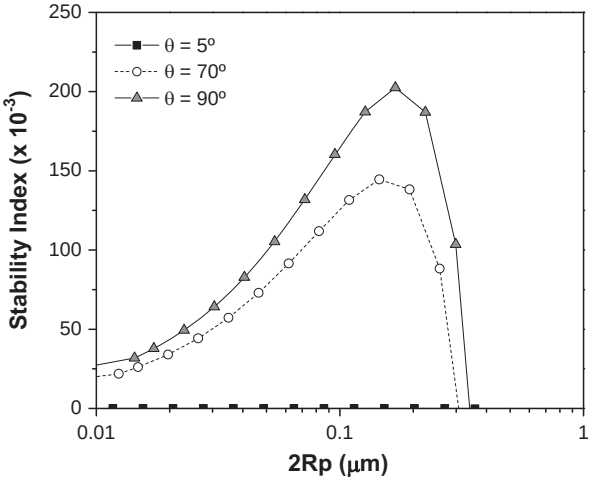

Fig. 8. Stability index as a function of the particle diameter for a bubble diameter ($2R_B$) of 0.1 μm, for different θ values. The other variables were kept the same as stated in Fig. 7.

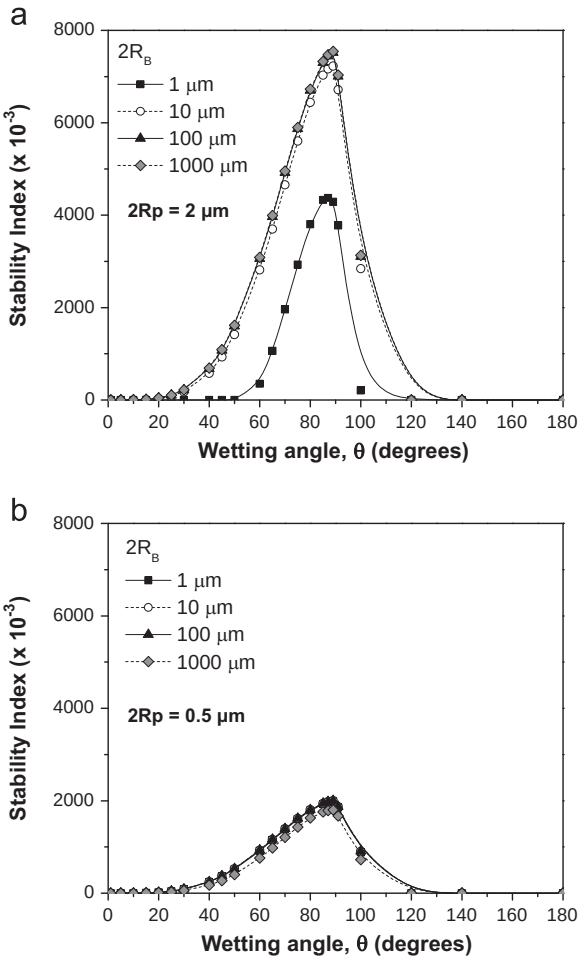

Fig. 9. Stability index as a function of the particle contact angle (θ) and of the bubble diameter. The particle size was fixed at 2 μm in (a) and 0.5 μm in (b). The other variables were kept the same as in Fig. 7.

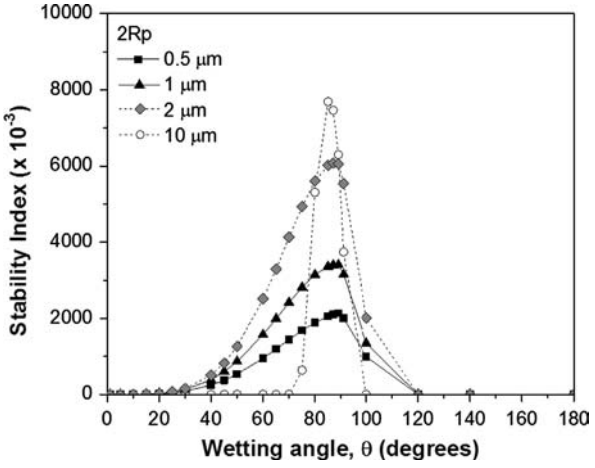

Fig. 10. Stability index based on Eq. (5) as a function of the particle contact angle (θ) and of the particle diameter for $2R_B = 10$ μm. The other variables were kept the same as in Fig. 7.

associated with particle containing foams, based on the following aspects:

I. The index is able to show a threshold for the particle size, as defined by the $P_{C\,max} - \Delta P_{eff}$ relationship.

II. It is also capable to address the interfacial stability aspect, as defined by the adsorption energy normalized by the thermal energy $\Delta G_{ads}/K_B T$ ratio.

5. Processing road maps for ceramic foams

In this section, the validity of the stability index, defined by Eq. (5), was compared to experimental results in the literature. Therefore, specific publications were selected where all physical properties required for evaluating $P_{C\,max}$, ΔP_{eff} and $\Delta G_{ads}/K_B T$ parameters were available.

The proposed stability index should be suitable to describe foam and foam-like systems that have the following features:

- Considerably high volumetric fraction of particles in the suspension prior to foaming, as the $P_{C\,max}$ equation assumes that there is some sort of structure formed by the particles within the bubble's film. This condition is only attained when the volumetric fraction of particles is above (> 10 vol% [17]).
- Narrow particle size distribution, due to the dependency of $P_{C\,max}$ upon the particle size (R_p, see Eq. (1)).

In this work, a novel way to analyze the stability and foam capacity of a system is proposed by the "Processing Road Maps" containing the stability index (Eq. (5)) and the inverse of suspension viscosity prior foaming ($1/\eta$) in the Y and X axes, respectively. Therefore, in order to draw the road map, all variables contained in the stability index equation and the suspension viscosity must be known. At the moment only a few studies have measured or estimated all those parameters [9,15,18]. Fig. 11 shows the example of a map which was built up using both calculated (stability index) and experimental ($1/\eta$) data found in the literature (all related to aqueous systems containing polymeric or ceramic particles). The incorporated air volume fraction, P (%), related to each system is indicated close to each point.

Fig. 11 is the first attempt to generate a generic tool that could be used to identify whether a particulate system can or not result in suitable foams. It is also a practical way to visualize the general scenario of particle stabilized foams as it reveals information of quite different systems containing: (1) polymeric particles and distinct solids content, (2) ceramic particles, (3) changes in the suspension ionic strength, and (4) hydrophobic modifiers. As shown in Fig. 11, there are regions in the graph where foaminess/stability is assured (indicated as (i)) and others where it is practically impossible (indicated as (ii)), when foam is prepared by *mechanical frothing*. Between those two regions, there is a "transition zone" which depends on the type of particles and the mechanism chosen to increase viscosity. When moving from the transition zone to the (ii) one, the P results decrease for low stability index (system 2) or for low $1/\eta$ values (systems 1 and 3). Those examples are discussed with more details below.

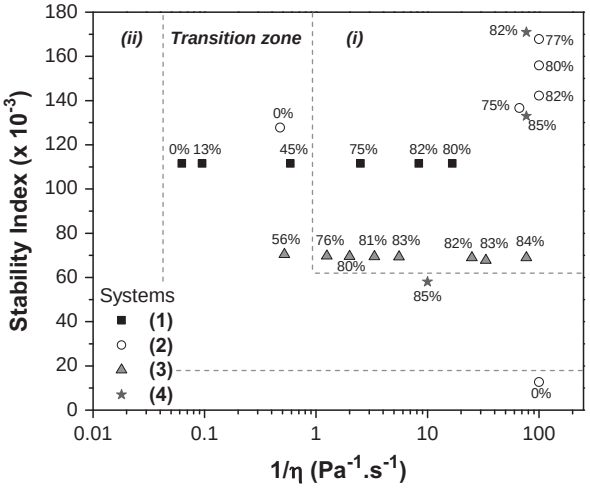

Fig. 11. Processing road maps for particle stabilized foams prepared by mechanical frothing. The dotted lines are an attempt to define regions (i), (ii) and a "transition zone". The starting data with the lowest stability index for the system 4 is within the transition zone because this system shows bubble coarsening (an indicative of a lack of stability) even though its P value was quite high (85%). Data taken from [9,18–21].

Moreover, Fig. 11 validates the necessity of correlating a stability related parameter (stability index) with a rheological one (viscosity) in order to visualize the general behavior of a foam system, which was the main goal in Fig. 1. Such argument is exemplified through systems 1 and 3 whose data points display approximately the same stability index value, although the foaminess (P) observed experimentally was quite different and dependent upon the suspension viscosity (a methodological constraint).

The great advantage of such a road map is the possibility of focusing on the future development of foams that are located in region (i). In order to do so, the physical properties are required to calculate the stability index and the suspension viscosity must be measured and controlled. Besides that, it is also possible to design systems that, a priori, should have suitable physical and rheological properties, which can minimize the chances of failure in the foam production.

5.1. Polymeric particles containing foams (system 1)

Polyvinilidene fluoride (PVDF) foam containing particles were considered based on Wong et al. [19] data that produced foams by adding 9 vol% alcohol to an aqueous suspension. In this study, the wetting angle of the particles (θ) and the liquid–gas interface tension (γ) were fixed at 62° and 42 mN/m, respectively, and the only parameter investigated was the variation of the volumetric fraction (vol%) of 0.25 μm sized PVDF particles. Fig. 11 shows that P values were extensively reduced for system 1 samples as η increased above critical values. It must be highlighted that the foams prepared by Wong et al. [19] were generated through mechanical frothing, a technique that requires low

viscosity values to allow air incorporation. Thus, the changes in the suspension viscosity are related only to the increase in the volumetric concentration of particles, which was varied from 6 up to 35 vol%.

It is observed that the calculated values for the stability index remained constant ($\sim 115 \times 10^{-3}$) for all PVDF foams, which indicates that each of those systems could generate stable foams. Nevertheless, the viscosity values were too high for the suspensions with high volumetric fraction of particles (points inside the transition zone), which prevented air from been incorporated. A possible way to clear out this feature would be to generate foams with the high viscosity ($1/\eta < 1\ \mathrm{Pa^{-1}\,s^{-1}}$) systems and analyze their foaminess/stability. The air incorporation would have to be forced by bubbling pressurized air inside the suspension. The results presented in Fig. 11 clearly state the importance of the methodology used to induce air incorporation. Therefore, if there is a rheological variable preventing that from occurring (viscosity, in this case), then the stability index value will not prevail. Nonetheless, with suitable rheological properties or by changing the method to incorporate air (by using pressurized air or by adding gas through a chemical reaction, for example) than the stability index dictates the foam behavior.

5.2. Ceramic particles containing foams (system 2)

The stability index was also calculated for ceramic foams produced by adding different amounts of valeric acid into a 200 nm and 35 vol% alumina suspension [18,20] whose results are shown in Fig. 11 with the corresponding suspension viscosity. In this case, the valeric acid is adsorbed on the alumina particles surface decreasing their hydrophilic behavior. Therefore, they become only partially wet by the water due to the increase in the θ value, which allows their adsorption in the air–water interface and, thus affecting the foam generation likelihood. Besides that, the valeric acid concentration scales with the suspension viscosity.

Fig. 11 shows two interesting aspects: by using 1 mmol/L (lower viscosity) and 50 mmol/L (higher viscosity) of valeric acid concentration, it was not possible to produce foams (points with $P=0\%$, located at the transition zone and region (ii)), whereas the intermediate concentrations resulted in quite high P values (75–82%). For the 1 mmol/L amount (lower viscosity), the value of the stability index attained is roughly 10 times lower than for the other systems. On the other hand, for 50 mmol/L content (highest viscosity: $1/\eta \sim 0.4\ \mathrm{Pa^{-1}\,s^{-1}}$), it shows a high stability index value and, yet, no foam could be produced. The latter behavior needs to be understood by the suspension viscosity (η) value, which was the highest for this system. Additionally, the gas had to be incorporated by mechanical frothing, that associated with the high viscosity, made the foam generation impossible. If the gas incorporation would have been carried out by another method, the stability of the foam might have been suitable. This latter analysis is analogous to what happened to the PVDF foam discussed before.

5.3. System 3

Fig. 11 also presents the stability index and viscosity values for alumina foams stabilized with propionic acid and modified by adding NaCl [20]. The evaluated propionic acid concentration was kept constant at 176 mmol/L.

In order to carry out the calculations, the wetting angle for propionic acid modified alumina was taken from elsewhere [21] and it was fixed at 42°, assuming that the NaCl concentration has very little effect on it. Besides that, the f and z values were considered 0.9 and 0.405, respectively.

Similarly to the PVDF and valeric acid modified alumina foams discussed before, the stability index alone cannot explain the reason for the diminishing values of P as the NaCl concentration increases. As the index remains high, the suspension viscosity must be the cause for the decrease in P values. That hypothesis is also confirmed by Fig. 11, which shows that as the alumina suspension viscosity increases above approximately 0.8 Pa s ($1/\eta = 1.25\ \mathrm{Pa^{-1}\,s^{-1}}$), P tends to decrease.

When one compares the effect of increasing suspension viscosity by increasing the alumina modifier (such as valeric acid, see Section 5.2) and by adding ionic electrolyte, it can be concluded that the foams produced by NaCl addition can result in higher P values (given the same viscosity) in the high viscosity range ($1/\eta < 2\ \mathrm{Pa^{-1}\,s^{-1}}$). That fact can be illustrated by observing that a suspension containing NaCl with viscosity of approximately 2 Pa s could induce the generation of foam with $P=56\%$ (Fig. 11). On the other hand, the suspension produced by increasing valeric acid (system 2) could not generate foams at all (0%) for the same viscosity value. This explanation reflects a real decoupling from the stability index and the viscosity, as the former system (NaCl) showed an index value of 70 and the latter (valeric acid) of 128, showing that the way in which viscosity is increased also matters or that, maybe, another rheological parameter could be more suitable for defining a threshold for air incorporation in mechanical frothing. For example, valeric acid reduces the repulsion between alumina particles by a hydrophobic effect [22] causing intense gelification in the system. On the other hand, the increase in the ionic strength does not lead to such a significant effect (this is only a hypothesis, as one would have to carry out G' and G'' measurements to confirm such a claim, or, at least, compare the entire viscosity–shear rate curve). The intense gelification usually happens because the short chain carboxylic acids cause a dramatic reduction in the zeta potential, which allows particle attraction to take place.

Nevertheless, the viscosity threshold above which the values of P begin to decrease is not too different for the two systems (2 and 3), as for the NaCl one it is about 0.8 Pa s ($1/\eta = 1.25\ \mathrm{Pa^{-1}\,s^{-1}}$) and for the valeric acid

system it is close to 0.3 Pa s ($1/\eta \sim 3\ Pa^{-1}\ s^{-1}$) [17] and that is the reason why those spots are located close to the transition zone in Fig. 11. Furthermore, in the PVDF foams (system 1) the threshold value of approximately 0.5 Pa s was also observed, as foams with higher viscosity resulted in smaller P values. Note that all those points are inside the transition zone in Fig. 11, indicating that even higher viscosity values would completely inhibit the foam formation.

5.4. System 4

Gonzenbach et al. [18] evaluated various surface modifiers (propionic acid, valeric acid and enanthic acid) to produce foams of alumina suspensions containing 200 nm particles and 35 vol% solid loading. The stability index was calculated and is presented in Fig. 11 with their respective viscosity values.

Based on P values shown in Fig. 11 the foams produced by such carboxylic acids modifiers are all in the same range (82–85%). However, Gonzenbach et al. [18] also evaluated the long-term stability of their systems by measuring the foam medium bubble size as a function of time and their values (the size measured at each time divided by the bubble size immediately after foaming) are presented in Fig. 12.

After 10 h the bubble size in the foams containing valeric and enantic acids were the same as just after foaming (relative size equals unity). On the other hand, the propionic acid foam showed some coarsening, as the bubbles more than doubled their initial values.

The results are presented in Fig. 11, where the point with the highest stability index (shown in the (i) zone and with $P=82\%$) represents the enantic acid system. The intermediate stability index value (also located in the (i) zone) represents the valeric acid containing foam and the lowest one (transition zone) the propionic acid system. It is also possible to notice that the viscosity of the enantic and valeric acid containing foams were similar, whereas for the propionic one it was higher.

The stability index associated to the valeric acid and enantic acid modified alumina foams were much higher (primarily due to the higher wetting angles) than the propionic acid foam, which can be related to the long-term kinetic stability of the systems and, thus, explaining the observed coarsening shown in Fig. 12. Therefore, there might be a minimum threshold for the stability index value that is necessary to attain in order to maintain long term stability, that is, to prevent bubble coarsening. As stated in the Fig. 11 caption, the first horizontal line of the transition zone was suggested based on the propionic acid system due to its lack of long-term stability.

Another very important remark is that coarsening took place in the propionic acid system even though its viscosity was *tenfold higher* than the other two, indicating that, for particle stabilized foams, viscosity may not be such an important kinetically influent parameter as it is in aqueous surfactant stabilized ones [23]. Additionally, in such systems the viscosity acts as a stabilizing element by slowing drainage and coalescence rates. Besides that, when increasing θ from 53° to 70°, a small effect in the 200 nm alumina foam formation should be verified, as the particle size of alumina in that case was very small. However, for larger particles, (3–7 μm), the effect of θ could be much more significant, as calculated by Eq. (5) and shown in Fig. 13.

Fig. 13 shows that for 5 μm particles, increasing θ from 50° to 70° allows the presence of 50 μm bubbles in the foam (as for $\theta=50°$ the stability index value associated with such particles is *zero*), meaning a much more "active" role of the wetting angle. In case one must generate a foam with a wide particle size distribution and, thus, the possible presence of bigger particles, the results shown in Fig. 13 might indicate that increasing θ close to the 70–80° range

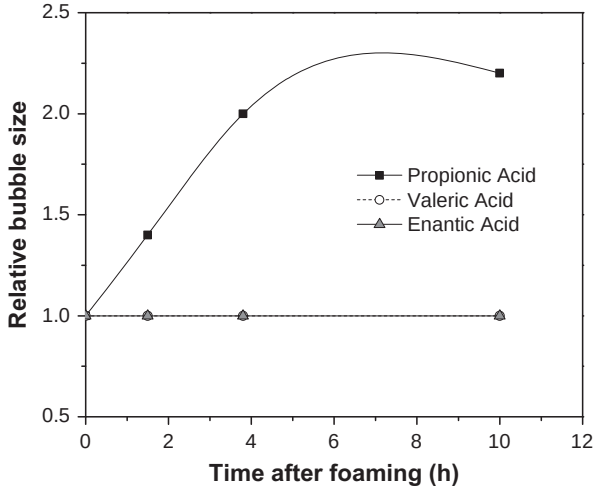

Fig. 12. Relative medium bubble size as a function of time (h) for foams containing the three surface modifiers [18].

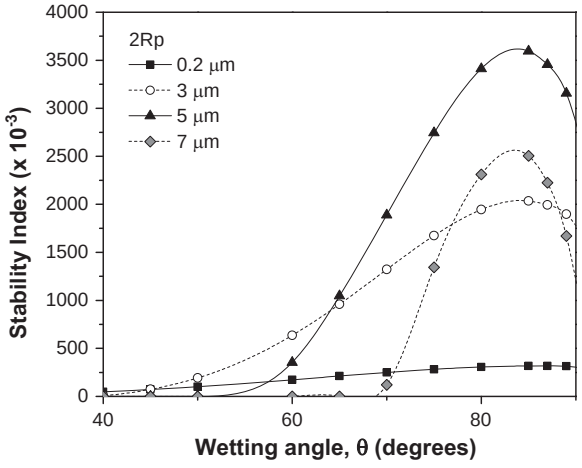

Fig. 13. Stability index as a function of θ and of the suspension particle size. For the calculations, the following values were used: $f=0.9$, $z=0.405$, $\gamma=0.06$ N/m, $2R_B=50$ μm.

might be vital for producing foams (otherwise, the large particles may act as potential foam disrupters).

6. Final remarks

The stability index derived in Section 4 (Eq. (5)) has the potential to become an indicative way to analyze different types of particle stabilized foams (Y axis of Fig. 1). When compared to the reciprocal of the suspension viscosity (X axis of Fig. 1) the stability index model expands the scientific understanding regarding such systems, especially because the previous ones [3,24,25] are not able to incorporate all variables in a single equation.

Some of the most important conclusions and insights that can be drawn are the following:

- The rash assumption that high suspension viscosity inhibits particle-containing foams generation must be reevaluated, as this is only true when mechanical frothing is selected for the manufacturing process. Even in that case, some results point out that the viscosity threshold may not be fully understood by merely comparing the suspension viscosity, as other rheological properties (such as G' and G'') may also be important and further investigations are still required. That fact is the possible cause of the uncertainty in the position of the maximum viscosity threshold in the road map (Fig. 11).
- The present model helps to generate insights about future processing trends in such systems. For example, the calculations showed that the wetting angle is (given a fixed particle size) the single most important parameter that controls foam stability/foamability. Besides that, the wetting angle influence is more significant for larger particles. Finally, the stability index was also able to explain the long-term stability of foams generated with different chemical modifiers, as lower index value was correlated to bubble coarsening (although adequate foaminess was attained).
- Although many literature results point out the validity of the proposed model, there are limitations (such as the maximum particle size) that still need further improvement regarding the predictions of the stability index.

The road map concept seems to be able to clarify the processing of foams by highlighting the likelihood of foam production and its stability. This tool allows the simultaneous visualization of a huge amount of information regarding physical properties (stability index and viscosity) with the systems goals (P, for example). However, its great drawback is that its conclusions are different for each processing method, as each one might result in different positions for the transition zone (for example, if air is injected under pressure in the system, then most likely the threshold for the maximum viscosity is increased). Nonetheless, it is possible to state that such a tool is a great advance to understand and control foam and foam-like systems.

Acknowledgments

The authors are grateful to the Brazilian research funding institution CNPQ, FIPAI and Federation for International Refractory Research and Education (FIRE) for supporting this work.

References

[1] T.X. Zhu, K. Coley, G. Irons, Progress in slag foaming in metallurgical processes, Metallurgical and Materials Transactions B 43 (2012) 751–757.
[2] A.R. Studart, U.T. Gonzenbach, E. Tervoort, L.J. Gauckler, Processing routes to macroporous ceramics: a review, Journal of American Ceramic Society 89 (2006) 1771–1789.
[3] G. Kaptay, Interfacial criteria for stabilization of liquid foams by solid particles, Colloids and Surfaces A: Physicochemical and Engineering Aspects 230 (2003) 67–80.
[4] P. Kruglyakov, A. Nushtayeva, Emulsions stabilised by solid particles—the role of capillary pressure in the emulsion films, in: D. Petsev (Ed.), Emulsions: Structure, Stability and Interactions, 1st ed., Elsevier, Amsterdam, 2004, pp. 671–677.
[5] R. Aveyard, J.H. Clint, T.S. Horozov, Aspects of the stabilization of emulsions by solid particles: effects of line tension and monolayer curvature energy, Physical Chemistry Chemical Physics 5 (2003) 2398–2409.
[6] M.F. Ashby, Materials Selection in Mechanical design, 3rd ed., Butterworth-Heinemann, Oxford, 2005, p. 512.
[7] N.D. Denkov, L.B. Ivanov, P.A. Kralchevsky, A possible mechanism of stabilization of emulsions by solid particles, Journal of Colloid and Interface Science 150 (1992) 589–593.
[8] G. Kaptay, On the equation of the maximum capillary pressure induced by solid particles to stabilize emulsions and foams and on the emulsion stability diagrams, Colloids and Surfaces A: Physicochemical and Engineering Aspects 282–283 (2006) 387–401.
[9] U.T. Gonzenbach, A.R. Studart, E. Tervoort, L.J. Gauckler, Stabilization of foams with inorganic colloidal particles, Langmuir 22 (2006) 10983–10988.
[10] D.O. Vivaldini, V.R. Salvini, A. Mourão, V.C. Pandolfelli, Unified critical geometry theory of particle-stabilized foams, in preparation.
[11] B. Binks, Particles as surfactants: similarities and differences, Current Opinion in Colloid & Interface Science 7 (2002) 21–41.
[12] M. Haw, Colloidal suspensions, Brownian motion, molecular reality: a short history, Journal of Physics: Condensed Matter 14 (2002) 7769–7779.
[13] S. Blundell, K. Blundell, Concepts in Thermal Physics, Oxford University Press, Oxford, 2006, p. 366.
[14] S.K. Bindal, G. Sethumadhavan, A.D. Nikolov e, D.T. Wasan, Foaming mechanisms in surfactant free particle suspensions, Materials, Interfaces, and Electrochemical Phenomena 48 (2002) 2307–2314.
[15] B. I., R. Pugh, J. van de Pas, I. Callaghan, Silica nanoparticle sols 1. Surface chemical characterization and evaluation of the foam generation (foamability), Journal of Colloid and Interface Science 313 (2007) 645–655.
[16] R. Feynman, QED: The Strange Theory of Light and Matter, Princeton University Press, Princeton, 2006, pp. 36–76.
[17] L. Gauckler, A.R. Studart, E. Tervoort, U.T. Gonzenbach, I. Akartuna, Ultrastable Particle-Stabilized Foams and Emulsions, Patent WO 2007/068127 A1, 21 June 2007.
[18] U.T. Gonzenbach, A.R. Studart, E. Tervoort e, L.J. Gauckler, Macroporous ceramics from particle-stabilized wet foams, Journal of American Ceramic Society 90 (2007) 16–22.

[19] J. Wong, E. Tervoort, S. Busato, Y. Gonzenbach, A. Studart, P. Ermanni, L. Gauckler, Designing macroporous polymers from particle-stabilized foams, Journal of Materials Chemistry 20 (2010) 5628–5640.
[20] U.T. Gonzenbach, A.R. Studart, E. Tervoort, L.J. Gauckler, Tailoring the microstructure of particle-stabilized wet foams, Langmuir 23 (2007) 1025–1032.
[21] D. Megias-Alguacil, E. Tervoort, C. Cattin, L. Gauckler, Contact angle and adsorption behavior of carboxylic acids on α-Al_2O_3 surfaces, Journal of Colloid and Interface Science 353 (2011) 512–518.
[22] A.R. Studart, R. Libanori, A. Moreno, U. Gonzenbach, T. E., L. Gauckler, Unifying model for the electrokinetic and phase behavior of aqueous suspensions containing short and long amphiphiles, Langmuir 27 (2011) 11835–11844.
[23] L. Brush, S. Davis, A new law of thinning in foam dynamics, Journal of Fluid Mechanics 534 (2005) 227–236.
[24] P. Kruglyakov, A. Nushtayeva, Investigation of the influence of capillary pressure on stability of a thin layer emulsion stabilized by solid particles, Colloids and Surfaces A: Physicochemical and Engineering Aspects 263 (2005) 330–335.
[25] P. Stevenson, Foam Engineering, 1st ed., John Wiley & Sons, West Sussex, 2012, pp. 121–138.